Infrared Multiphoton Dissociation Mechanism of 1,2-Dichlorotrifluoroethane in a Molecular Beam

Atsushi Yokoyama,* Keiichi Yokoyama, and Ginji Fujisawa

Advanced Science Research Center, Japan Atomic Energy Research Institute, Tokai-mura, Naka-gun, Ibaraki 319-11

(Received May 18, 1995)

The mechanism of the infrared multiphoton dissociation of the title molecule has been studied using photofragmentation translational spectroscopy. The HCl elimination and the C–Cl bond rupture occurred competitively as primary dissociation channels. The HCl elimination reaction accounts for 66^{+5}_{-9}% of the total primary dissociation yields at 16±3 J cm^{-2}. This is consistent with the branching ratio calculated by RRKM theory. A C=C bond rupture of the CF_2CFCl molecules and C–Cl bond rupture of C_2HF_3Cl radicals were also observed as secondary photodissociation processes. The average excitation energy of the dissociating 1,2-dichlorotrifluoroethane molecules was found to be 14—36 kcal mol^{-1} (1 kcal mol^{-1}=4.184 kJ mol^{-1}) above the C–Cl dissociation threshold of the molecules by comparing the observed center-of-mass translational energy distribution for the C–Cl bond rupture with that calculated by Rice–Ramsperger–Kassel–Marcus (RRKM) theory.

Infrared multiphoton absorption (IRMPA) and subsequent dissociation (IRMPD) of polyatomic molecules have received much attention over the past two decades. Their mechanisms and dynamics[1] and their application to laser isotope separation[2] have attracted the interest of several researchers.

In the IRMPD of chlorinated and/or fluorinated hydrocarbons several primary dissociation pathways, such as HCl, Cl, Cl_2, and HF eliminations, have been observed. In some large molecules, a few dissociation pathways occurred competitively. For example, the competitive C–Cl bond rupture and HCl elimination have been observed in the IRMPD of CF_3CHClF[3,4] and CCl_2CHCl.[5] The C–Cl bond rupture and the Cl_2 eliminations occurred competitively in the IRMPD of CF_2Cl_2.[6] The competitive HCl and HF eliminations have been observed in the IRMPD of $CHClFCHClF$[7] and $CClF_2CH_2Cl$.[8] In the case of the IRMPD of CF_3CH_2Cl, C–Cl bond rupture, HCl and HF eliminations occurred competitively.[9] At relatively high laser fluence, secondary photodissociations of primary products have also been observed in some cases. Such secondary photodissociation complicates the estimate of the dissociation mechanism from the analysis of the final products.

Photofragmentation translational spectroscopy (PTS) is a powerful technique for studying the dissociation mechanism of a complex system undergoing several primary and/or secondary dissociation processes like those described above, because the dissociation products can be detected directly under collision-free conditions. The PTS has been successfully applied to the studies of the IRMPD of many halogenated hydrocarbons.[3,5,6,10—13]

In the IRMPD of 1,2-dichlorotrifluoroethane (1,2-DCTFE), Lupo et al. observed chlorotrifluoroethylene, trifluoroethylene, and 1,2-dichlorodifluoroethylene as main products in the ratio 6:4:1 at the laser fluence of 4 J cm^{-2}. They concluded that 1,2-DCTFE dissociates competitively through HCl, HF, and Cl_2 elimination reactions.[14] However, trifluoroethylene may be produced not from the Cl_2 elimination reaction but from the successive C–Cl bond ruptures. The purpose of this study is to elucidate the reaction mechanism of the IRMPD of 1,2-DCTFE by using the PTS.

Experimental

Experimental Procedure and Ab Initio Calculations. A molecular beam machine for the PTS is described in detail elsewhere.[3] The molecular beam was formed by expanding 200 Torr of 1,2-DCTFE (PCR Research Chemicals) (1 Torr=133.322 Pa) into the source region through a 0.1 mm diam. nozzle. The nozzle was heated at 280 °C to enhance multiphoton absorption and to prevent the formation of clusters. The molecular beam was collimated by being passed through two skimmers and was crossed with the laser beam at the center of the main region. The laser beam from a TEA CO_2 laser (Lumonics TEA-841) with a temporary pulse form of a 100 ns spike followed by 5 μs tail was focused with a 30 cm focal length ZnSe lens. The size of the laser spot was 3×3 mm^2 at the interaction region of the laser and the molecular beam. The 1,2-DCTFE was excited at 9.504 μm with the laser fluence of 16±3 J cm^{-2}. The neutral fragments flew into an ionizer of a triply differentially pumped quadrupole mass-spectrometer (EXTREL C-50), located at 44.0 cm away from the interaction region. These fragments

were ionized with electron bombardment at 100 eV of the electron energy, mass-selected by a quadrupole mass spectrometer and were detected by a secondary electron multiplier. The time-of-flight (TOF) spectra of the fragments were recorded on a multichannel scaler triggered by a pulse synchronized with the laser pulse. Signals in each TOF spectrum were accumulated over 100000—1200000 laser shots. The spectra were obtained at 10° of the beam-to-detector angle which is defined as the angle between the molecular beam axis and the detector axis. Since the angular distributions of fragments in the center-of-mass (c.m.) frame are essentially isotropic in the IRMPD,[6] the relative concentrations of the fragments can be obtained from the signal intensities at only one beam-to-detector angle. The velocity distribution of the molecular beam was measured by a conventional TOF method. The molecular beam was chopped to ca. 12 μs pulse by a slotted wheel and the TOF spectra of the molecular beam were measured at the beam-to-detector angle of 0°. The number density distribution of the beam velocity $f(v)$ is well represented by the following formula:

$$f(v) = Av^2 \exp\left[-\{(v/\alpha) - S\}^2\right],$$

where A is a normalization constant, α=158 m s^{-1} and S=3.36.

The ion flight time from the ionizer to the detector was subtracted from the measured flight time to obtain the true molecular flight time. The ion flight time t_{ion} was calculated by the equation:

$$t_{ion} = \alpha_{ion}\sqrt{M}$$

where M is the ion mass in units of amu. The proportional constant α_{ion} was determined to be 4.15 from the plot of the peak flight times in the TOF spectra of the fragment ions of the 1,2-DCTFE as a function of $\sqrt{M}$.

In order to estimate the potential energies of the reactions observed, we have done ab initio molecular orbital calculations. The energies and stationary point geometries were calculated at the MP2 level of theory. Wadt and Hay's effective core potentials[15] accompanied with split valence plus polarization functions (ECPDZP) were used as basis functions, except for the minimum energy path calculation of the C–Cl bond rupture of the C_2HClF_3 radical. In that case, 6-31G** functions were used. All calculations were carried out using a GAUSSIAN 90 program.[16]

Results and Analysis

Signals of fragments were detected at $m/z = 31$ (CF^+), 32 (CHF^+), 35 (Cl^+), 36 (HCl^+), 50 (CF_2^+), 66 ($CClF^+$), and 82 ($C_2HF_3^+$). In these ions, the CHF^+ signal is weak, so we did not analyze the TOF spectrum at m/z=32. Since the peak flight time after the subtruction of the ion flight time is almost same as that of the TOF spectrum at m/z=82, both CHF^+ and $C_2HF_3^+$ ions should come from the same dissociation product.

A. HCl Eliminations. The TOF spectrum of HCl^+ is shown in Fig. 1. This signal must come from HCl produced by the following HCl elimination reactions:

$$CClF_2CHClF \rightarrow CF_2ClCF + HCl \quad (1a)$$

$$CF_2CFCl + HCl \quad (1b)$$

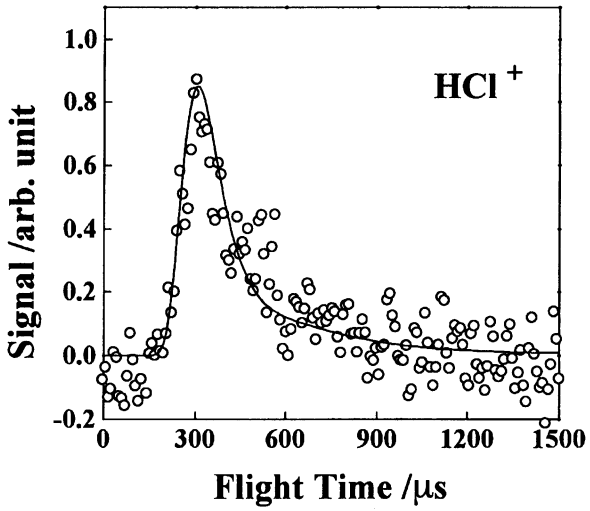

Fig. 1. TOF spectrum at m/z=36. Open circles represent experimental data and the solid line shows the best fit.

Since 1,2-DCTFE has two Cl atoms attached to different carbon atoms, three-centered HCl elimination [reaction (1a)] and/or four-centered HCl elimination [reaction (1b)] may occur. The threshold energies for reactions (1a) and (1b) are calculated to be 77.0 and 77.9 kcal mol^{-1} by the ab initio MO calculations, respectively. Although the exit barrier is typically much higher for the four-centered HCl elimination than for the three-centered HCl elimination, the average translational energies released from both reactions are almost the same because of low conversion fraction (10—20%) of the exit barrier to the translational energy of the products for the four-centered HCl elimination.[11] Although HCl molecules produced by reactions (1a) and (1b) are not resolved from each other on the TOF spectra, we think from the theoretical energies that both reactions can occur. Figure 2 shows the c.m. translational energy distribution $P(E)$ for reaction (1). This $P(E)$ was determined from the fit of the HCl^+ TOF spectrum by a forward convolution method.[17] The peak and average energies of the $P(E)$ are 3.6 and 4.9 kcal mol^{-1}, respectively.

B. C–Cl Bond Ruptures. Since Cl atoms were observed in the Cl^+ TOF spectrum, it is certain that the following C–Cl bond ruptures occurred:

$$CClF_2CHClF \rightarrow CF_2ClCHF + Cl \quad (2a)$$

$$CF_2CHClF + Cl \quad (2b)$$

The counterpart of Cl, i.e., C_2HClF_3, should appear in the $C_2HF_3^+$ TOF spectrum. If no secondary C–Cl rupture of C_2HClF_3 produced by reaction (2) occurred, both Cl^+ and $C_2HF_3^+$ TOF spectra should be simultaneously fit only with reaction (2) by taking the conservation of linear momentum into account. At first, the Cl^+ TOF spectrum was fit only with reactions (1) and (2), as shown in Fig. 3(a). Then the contribution of

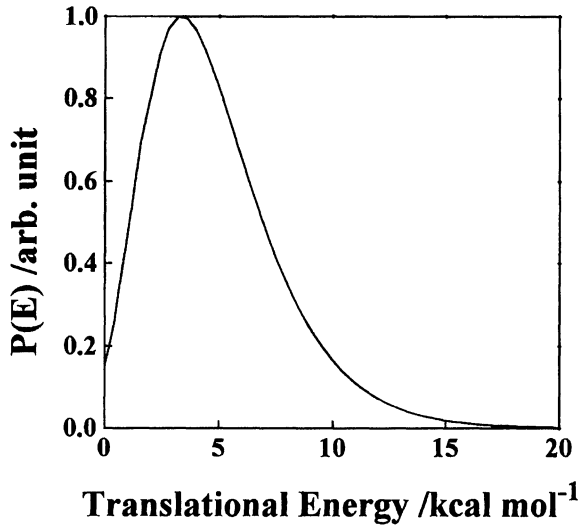

Fig. 2. C.m. translational energy distribution for the HCl elimination from 1,2-DCTFE.

C_2HClF_3 from reaction (2) was simulated by using the $P(E)$ determined by the fit of the Cl^+ TOF spectrum. However, the momentum matching is poor in this system, as shown in Fig. 3(b). The fast component drawn by the dotted line in the Cl^+ TOF spectrum represents the Cl^+ ions produced by the electron bombardment of HCl in the ionizer. The shape and the flight time of this component are the same as in the HCl^+ TOF spectrum in Fig. 1. The fragmentation of the dissociation products during electron impact ionization, such as the C_2HF_3Cl radical to the $C_2HF_3^+$ ion and the HCl molecules to the Cl^+ ions by the electron bombardment at 100 eV, does not alter the velocity of the fragments, according to our experimental experience.[3,12,13] For example, in the IRMPD of $CBrF_2CHBrF$, both Br^+ and $C_2HF_3^+$ TOF spectra could be simultaniously fit well with the $Br+C_2HBrF_3$ reaction.[12] Therefore, the failure of the momentum matching implies that the following C–Cl bond ruptures of C_2HClF_3 radicals also occurred:

$$CClF_2CHF \rightarrow CF_2CHF + Cl \quad (3a)$$

$$CF_2CHClF \rightarrow CF_2CHF + Cl \quad (3b)$$

The sequential carbon–halogen bond ruptures of polyhalogenated ethanes have also been observed in IRMPD of some polyhalogenated ethanes under similar experimental conditions.[12] Lupo and his co-workers[14] have also observed the stable C_2HF_3 molecules as one of the major products by IRMPD of 1,2-DCTFE in the bulb experiment. They suggested the occurrence of the following Cl_2 elimination:

$$CClF_2CHClF \rightarrow CF_2CHF + Cl_2 \quad (4)$$

Since no Cl_2^+ ion signal was observed and since both Cl^+ and $C_2HF_3^+$ TOF spectra could not be simultaneously fit with reaction (4), reaction (4) was not significant for us and the C_2HF_3 molecules were produced

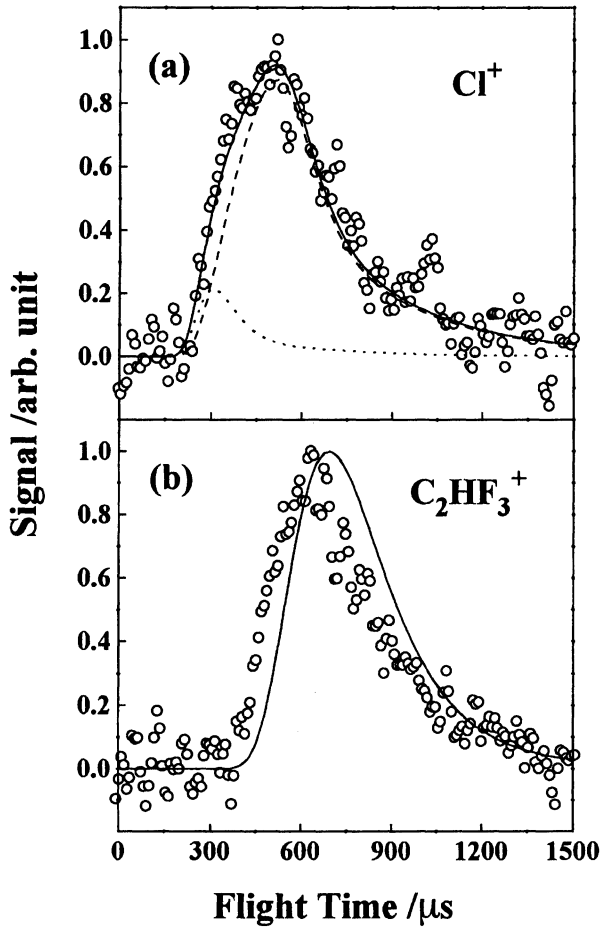

Fig. 3. TOF spectra. (a) $m/z=35$: — overall fit; ···· contribution of HCl from reaction (1); --- contribution of Cl from reaction (2). (b) $m/z=82$: — contribution of C_2HClF_3 from reaction (2) predicted by the momentum matching between Cl and C_2HClF_3. The poor fit indicates the existence of a reaction other than reaction (2).

through the sequential C–Cl bond ruptures [reactions (2) and (3)]. We confirmed that Cl_2 molecules could be detected as Cl_2^+ ions in our detection system by detecting the Cl_2 product from the IRMPD of CF_2Cl_2, where Cl_2 elimination and C–Cl bond rupture channels occur competitively with the branching ratio of 1 : 9.[6] Therefore, the Cl_2^+ ions would be observed in the IRMPD of 1,2-DCTFE, if the significant Cl_2 elimination were to occur, as suggested by Lupo et al. The C–Cl bond rupture of CF_2CFCl produced by reaction (1) is not significant, because the CF_2CFCl molecules produced by the sequential C–Br bond ruptures of $CBrF_2CBrClF$ dissociated to the CF_2 and CFCl radicals after the infrared multiphoton excitation; no evidence of the C–Cl bond rupture was observed.[5,18]

It is difficult to determine unambiguously the contributions of the products from reactions (2) and (3) in the Cl^+ and $C_2HF_3^+$ TOF spectra, because the two spectra show only one broad peak. We analyzed the

spectra as follows. The $P(E)$'s for reactions (2) and (3) were assumed to decay exponentially with the increase of the translational energy, except for the translational energy below 0.2 kcal mol^{-1} for reaction (2). The $P(E)$ decaying exponentially with the increase of the translational energy is very similar to that predicted by RRKM theory and generally observed for the reactions with no exit channel barrier.[3,10,12] The peak at 0.2 kcal mol^{-1} for the $P(E)$ for reaction (2) is needed for the slow part of the Cl^+ TOF spectrum to be fit well. This peak is probably due to the centrifugal barrier.[3] The number of Cl atoms from reaction (3) is equal to or less than that form reaction (2). This gives the upper limit of the ratio of the total counts of Cl atoms from reaction (3) to that from reaction (2) in the Cl^+ TOF spectrum. The ratio of the total counts of Cl atoms from reaction (3) to those from reaction (2) in the Cl^+ TOF spectrum can be calculated from the ratio of the number of Cl atoms produced by reaction (3) to those produced by reaction (2) by knowing the angular distribution of Cl in the c.m. frame.[17] Since the c.m. product angular distribution is essentially isotropic in IRMPD, we adopted this distribution in the analysis. As shown in Fig. 4, good fits were obtained by using the $P(E)$ with average energies from 1.5 to 3 kcal mol^{-1} for reaction (2) and the $P(E)$ with the corresponding average energy from 2.5 to 1.0 kcal mol^{-1} for reaction (3). It should be noted that the sum of the average energies for reactions (2) and (3) is about 4 kcal mol^{-1}. The $P(E)$'s are shown in Fig. 5. In these fits, the concentration of Cl atoms produced by reaction (3) is the same as that produced by reaction (2). This implies that all C_2HClF_3 radicals dissociated through reaction (3) and that the $C_2HF_3^+$ signal come only from C_2HF_3.

C. Secondary C–C Bond Rupture of CF_2CClF and HF Elimination from 1,2-DCTFE. Although signals from the counterparts of HCl, that is, CF_2CClF and/or $CClF_2CF$, were not observed, this is due to the following secondary dissociation of CF_2CFCl:[18]

$$CF_2CClF \rightarrow CF_2 + CClF \quad (5)$$

Since the 1,2-Cl migration in $CClF_2CF$,

$$CClF_2CF \rightarrow CF_2CClF, \quad (6)$$

occurs easily,[19,20] the $CClF_2CF$ from reaction (1a) dissociates through reaction (5) following the 1,2-Cl migration. Since the line center of the P branch of ν_4 mode for CF_2CClF coincides with the laser frequency and the CF_2CClF produced by reaction (1) is vibrationally excited, it can dissociate easily. The products produced by reaction (5) are observed in the CF^+, CF_2^+, and $CFCl^+$ TOF spectra as shown in Fig. 6. The translational energy distribution for reaction (5) determined by the fit of the TOF spectra is shown in Fig. 7. The average translational energy is 2.0 kcal mol^{-1}.

Lupo et al.[14] reported that the following HF elimi-

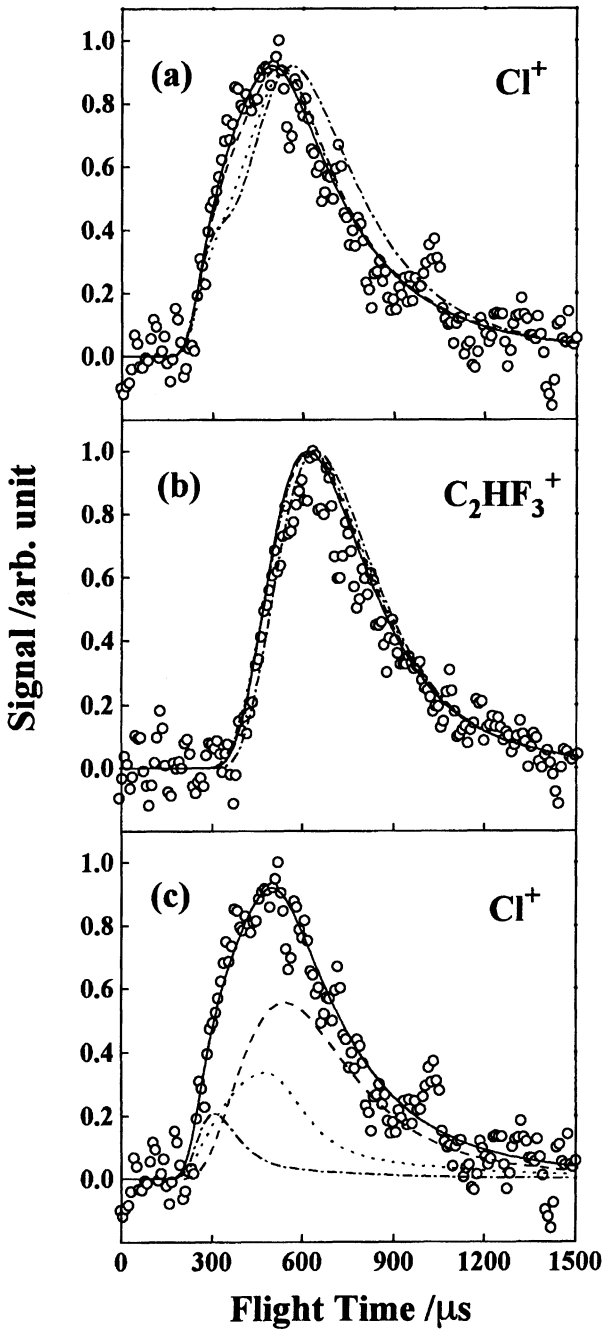

Fig. 4. The simulated TOF spectra. (a) m/z=35 and (b) m/z=82: Curves indicate the spectra calculated with different $P(E)$'s for reactions (2) and (3); ···· average energies of 1.0 kcal mol^{-1} for reaction (2) and 3.0 kcal mol^{-1} for reaction (3); - - - 1.5 kcal mol^{-1} for reaction (2) and 2.5 kcal mol^{-1} for reaction (3); — 3 kcal mol^{-1} for reaction (2) and 1.5 kcal mol^{-1} for reaction (3); -·- 3.5 kcal mol^{-1} for reaction (2) and 0.5 kcal mol^{-1} for reaction (3). (c) best fit of TOF spectrum obtained with the average energies of 3 kcal mol^{-1} for reaction (2) and 1.5 kcal mol^{-1} for reaction (3) at m/z=35: -·- contribution of HCl from reaction (1); - - - contribution of Cl from reaction (2); ···· contribution of Cl from reaction (3).

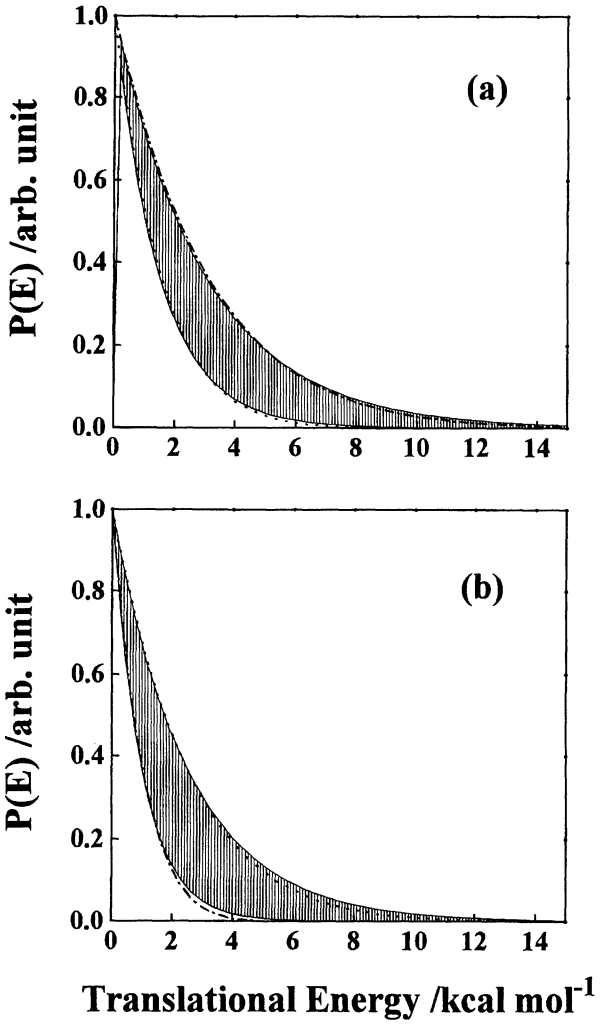

Fig. 5. C.m. translational energy distributions. The hatched areas show the ranges of uncertainty. (a) reaction (2): The dash-dotted and dotted curves represent the RRKM distributions with the average excess energies of 36 and 14 kcal mol^{-1}, respectively. (b) reaction (3): The dash-dotted and dotted curves represent the RRKM distributions with the average excess energies of 5 and 21 kcal mol^{-1}, respectively.

nation reaction also occurred:

$$CClF_2CHClF \rightarrow cis\text{-}CFClCFCl + HF \quad (7a)$$

$$\rightarrow trans\text{-}CFClCFCl + HF \quad (7b)$$

The HF product should be detected as HF^+ in our detection system as was observed in the HF elimination from CH_2CHF.[21] In the mass spectrum of the CFClCFCl molecule,[22] the primary ion is the most abundant. However, the fragment ions may be more abundant than the primary ion in the case of the mass spectra of the halogenated ethylenes produced by the IRMPD, because the product is expected to be vibrationally excited. Therefore, the *cis*-and/or *trans*-CFClCFCl products from reaction (7) should appear as $C_2F_2Cl_2^+$ and/or $C_2F_2Cl^+$ ions. We have carefully surveyed signals of HF^+, $C_2F_2Cl_2^+$, and $C_2F_2Cl^+$. However, no signal could be detected. Therefore, the HF elimination reaction should be a minor reaction process.

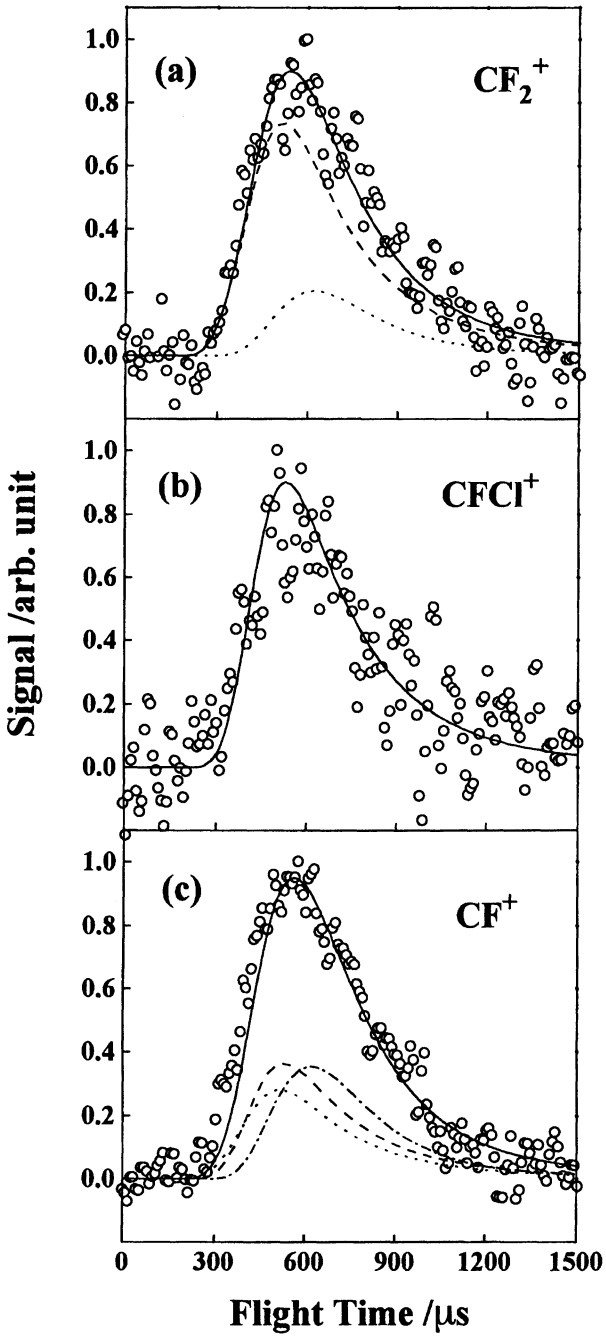

Fig. 6. TOF spectra. (a) m/z=50: --- contribution of CF_2 from reaction (5); ···· contribution of CF_2CHF from reaction (3). (b) m/z=66: — contribution of CFCl from reaction (5). (c) m/z=31: --- contribution of CFCl from reaction (5); ···· contribution of CF_2; -·- contribution of CF_2CHF.

D. Branching Ratio of the HCl Elimination to the C–Cl Bond Rupture. The branching ratio of the reaction (1) to reaction (2) is defined by the ratio

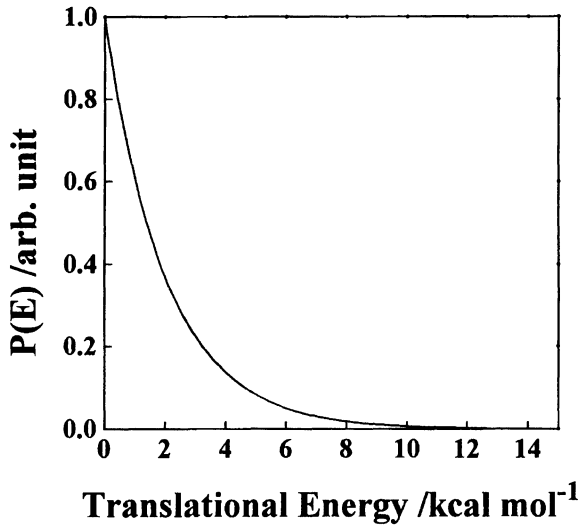

Fig. 7. C.m. translational energy distribution for reaction (5).

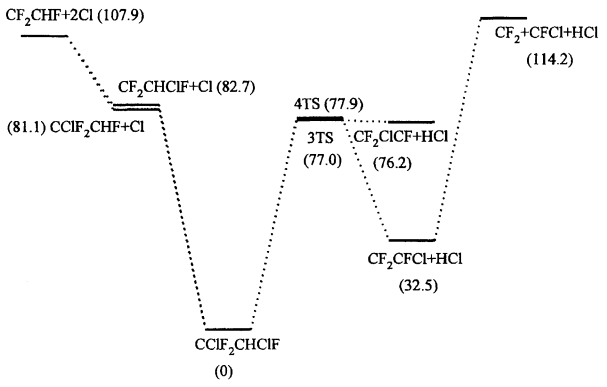

Fig. 8. Energy diagram for the reaction observed. Values in parentheses indicate the enthalpies of the reactions calculated at the MP2/ECPDZP level in unit of kcal mol^{-1}. 4TS and 3TS stand for the four- and three-centered transition states of the HCl elimination from 1,2-DCTFE, respectively.

of the HCl concentration to the Cl concentration and is determined to be about 1.9±0.6 from the total counts per one laser pulse of HCl and Cl from reaction (2) measured at the detector angle of 10° and at 16±3 J cm^{-2}. The procedure by which we got the true branching ratio from the ion signals measured in the mass spectrometer was the same as that described in Ref. 6. The relative ionization cross sections of HCl and Cl were calculated by the empirical form of the maximum ionization cross section:[6]

$$\alpha = 36\sqrt{\alpha} - 18$$

where α is the polarizability in unit of Å^3. The cross sections of most species reach a peak in the vicinity of 100 eV.[23,24] The values of the polarizabilities for Cl and HCl are 2.18[25] and 2.63,[26] respectively. The error in the branching ratio mainly comes from the error in the total signal counts of HCl, because the background is high at $m/z=36$. The error in the total counts was estimated to be ±29% by measuring three times the total signal counts per 400000 laser shots. The error associated with the uncertainty of the fraction of the Cl atoms produced by the primary C–Cl bond ruptures in the Cl^+ TOF spectrum is small (±5% of the branching ratio). The error associated with the correction for the relative ionization efficiency described above should be small, because the difference between the polarizabilities of HCl and Cl is small.

Lupo et al. observed the products C_2F_3Cl and C_2F_3H in the ratio 6:4 at the laser fluence of 4 J cm^{-2}. If the C_2F_3H was produced exclusively by the successive Cl atoms' elimination reactions (2) and (3), the branching ratio is 1.5 and is consistent with our value.

Discussion

The energy diagram for the reactions observed is shown in Fig. 8. The primary dissociation processes observed are the HCl elimination and the C–Cl bond rupture. Cl_2 elimination, which was suggested by Lupo et al.,[14] does not occur. Clearly, the CF_2CHF product observed by Lupo et al. comes from the sequential C–Cl bond rupture (reactions (2) and (3)). The threshold energy of a similar reaction, $C_2H_4F_2 \rightarrow C_2H_4+F_2$, is reported to be 115.7 kcal mol^{-1} from the ab initio calculation at the MP2/6-31+G level.[27] Therefore, the activation energy of the four-centered Cl_2 elimination should also be high, and the reaction could not occur competitively with the HCl elimination and the C–Cl bond rupture. The HF elimination from 1,2-DCTFE [reactions (7a) and (7b)] is not observed in this experiment either. The threshold energies for reactions (7a) and (7b) are calculated to be 81.9 and 80.9 kcal mol^{-1} by the ab initio calculation, respectively. The dissociation rates were calculated at various excitation energies by RRKM theory to examine the theoretical branching ratio for reaction (7). The details of the calculations are given in Appendix. The dissociation rates for the reactions observed and reaction (7) are plotted against excitation energy in Fig. 9. The dissociation rate for the HF elimination is calculated to be 1.8—3.7% of the total dissociation rate at 95—117 kcal mol^{-1}, which is the average excitation energy range of the dissociating 1,2-DCTFE described below. Therefore, this result is consistent with the fact that the products from reactions (7) could not be detected in this study. If the halogenated ethylenes observed by Lupo et al. come only from primary dissociation reactions, the yield of the $C_2F_2Cl_2$ molecule is 9% of the total dissociation yield. This value is rather larger than the calculated value. Therefore, the $C_2F_2Cl_2$ molecules may be produced by some secondary reactions.

The $P(E)$ for a simple bond rupture with no exit channel barrier is well reproduced by RRKM theory.[3,5,10,12] This characteristic allows us to estimate the average excitation energy of dissociating molecules.

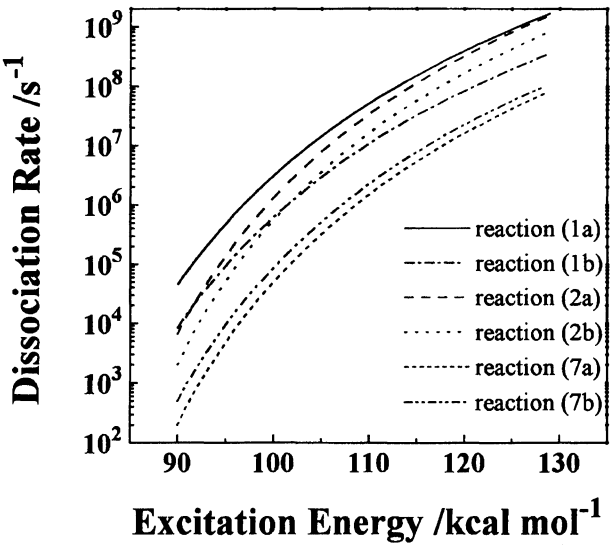

Fig. 9. RRKM dissociation rate constants for reactions (1), (2), and (7) as a function of the excitation energy.

In order to estimate the average excitation levels of the dissociating 1,2-DCTFE and CF_2ClCHF and the branching ratios for the reactions observed, we calculated the $P(E)$'s using the RRKM theory. The dissociation rates for reaction (2a) are 2.0—2.6 times as large as those for reaction (2b) because of the lower activation energy. Therefore, only the $P(E)$'s calculated for reactions (2a) and (3a) were compared with the observed $P(E)$'s. The calculated $P(E)$'s are shown in Fig. 5. From the comparison of the calculated $P(E)$'s with the observed ones, the average excitation levels of the dissociating $CClF_2CHClF$ and $CClF_2CHF$ are estimated to be about 14—36 and 5—21 kcal mol^{-1} above the dissociation energy of the corresponding C–Cl bond, respectively.

The branching ratio based on the RRKM rate constants decreases from 3.0 to 1.0 with the increase of the excitation energy of 1,2-DCTFE in the excitation energy range form 95 to 117 kcal mol^{-1}, which is the range estimated from the observed $P(E)$ of reaction (2). The RRKM branching ratio is consistent with the experimental value of 1.9±0.6.

The excitation energy of the dissociating 1,2-DCTFE which gives the same calculated branching ratio as that observed is about 101 kcal mol^{-1}. This value corresponds to an excess energy of 20 kcal mol^{-1} above the C–Cl dissociation threshold. So the average translational energy for reaction (2) is expected to be 2.0 kcal mol^{-1}. Since the sum of the average translational energies for reactions (2) and (3) is about 4 kcal mol^{-1}, the average translational energy for reaction (3) is expected to be 2.0 kcal mol^{-1}. Consequently, the average excitation energy of the CF_2ClCHF radical can be estimated to be 41 kcal mol^{-1} (14 kcal mol^{-1} above the C–Cl dissociation threshold of CF_2ClCHF). If we adopt these values, the CF_2ClCHF radicals have dissociated after the absorption of about 7 photons. The dissociation rate of 1,2-DCTFE via reaction (2a) at the excitation energy of 101 kcal mol^{-1} is about 2×10^6 s^{-1}. Therefore, most of the CF_2ClCHF radicals are produced within the laser pulse, and have a chance to absorb photons.

Conclusion

The IRMPD mechanism of 1,2-DCTFE has been studied by the PTS. The HCl and Cl eliminations have occurred competitively as the primary processes with the branching ratio of $0.66^{+0.05}_{-0.09}:0.34^{+0.09}_{-0.05}$. The average excitation energy of the dissociating 1,2-DCTFE has been determined to be 95—117 kcal mol^{-1} by the comparison of the observed c.m. translational energy for the Cl elimination with that calculated by the RRKM theory. The secondary photodissociation of the primary product C_2HClF_3 from the Cl elimination has also occurred via the C–Cl bond rupture of the C_2HClF_3 radical. The secondary photodissociation of the primary product CF_2CClF from the HCl elimination has also been observed.

Appendix: RRKM Calculations

The parameters used in the RRKM calculation are summarized in Table 1. For the C–Cl bond ruptures of 1,2-DCTFE, 15 vibrational frequencies of the transition state were taken from the frequencies of the corresponding halogenated ethyl radicals. The frequencies of the CF_2ClCFH and CF_2CHClF radicals were calculated at the MP2/ECPDZP and UHF/6-31G** levels, respectively. The two C–Cl bending frequencies of the transition states were determined by lowering the C–Cl bending frequencies of the 1,2-DCTFE so that $\log A=15.0$ at 1000 K, which is a typical value of the high-pressure A factor for the C–Cl bond rupture reaction. The moments of inertia of the transition states were calculated by assuming that the structures were the same as the 1,2-DCTFE molecule except that the breaking C–Cl bond length was 3.0 Å. The frequencies of 1,2-DCTFE, $CClF_2CHF$, and CF_2CHClF were calculated by the ab initio MO method. For the C–Cl bond rupture of $CClF_2CHF$, the frequencies and the structural geometry of the transition state were taken from the optimized geometry and the frequencies at the C–Cl bond length of 2.3 Å, at which there is a saddle point on the potential energy surface for the C–Cl bond rupture calculated by the ab initio MO method at the MP2/6-31G** level. In the ab initio MO calculation for the $C_2H_4Cl\rightarrow C_2H_4+Cl$ reaction at the HF/6-31G* and MP2/6-31G* levels of theory,[28] a saddle point was also observed at the C–Cl bond length of 2.6 Å. Although it is not certain whether the saddle point exists on the actual potential, an RRKM calculation for the rate constant of the $Cl+C_2H_2$ association reproduced well the experimental rate constants using a similar potential energy surface.[29] The frequencies and the geometries of 1,2-DCTFE, the transition states of the three- and four-centered HCl eliminations and the transition states of the four-centered HF eliminations were calculated by the ab initio MO theory at the MP2/ECPDZP//MP2/ECPDZP level. The

Table 1. Parameters Used for RRKM Calculations

1,2-DCTFE	$CClF_2CHF$	HCl elimination		C–Cl bond rupture			HF elimination	
		(1a)	(1b)	(2a)	(2b)	(3b)	(7a)	(7b)
			Frequency/cm^{-1}					
3074	3148	1537	1608	3148	2960	3001	1641	1643
1344	1382	1276	1440	1382	1382	1399	1428	1434
1272	1207	1199	1407	1207	1289	1299	1240	1239
1228	1143	1193	1206	1143	1249	1198	1178	1198
1134	1106	936	1107	1106	1196	1113	1052	1064
1085	1020	850	990	1020	1121	850	914	862
986	712	796	713	712	984	627	629	632
802	616	657	656	616	809	570	608	611
770	591	602	531	591	581	434	519	542
598	450	453	483	450	459	361	418	424
460	415	404	401	415	403	301	384	398
424	343	328	295	343	365	237	333	333
380	295	240	238	295	300	185	272	264
332	192	179	186	192	177	127	241	240
258	86	162	163	86	63		216	197
232		86	153	52	47		162	173
166		42	73	23			80	78
70								
			Moment of inertia/amu $Å^2$					
174	150	179	257	177	186	126	247	207
392	195	510	428	602	600	197	352	412
463	252	569	460	665	667	312	454	461
			Critical energy/kcal mol^{-1}					
		77.0	77.9	81.1	82.7	26.8	81.9	80.9

frequencies from the ab initio MO calculations were scaled by factors of 0.95 and 0.89 at the MP2 and UHF levels of theory, respectively, to correct the systematic errors in the calculated frequencies.[30)]

References

1) P. A. Schulz, Aa. S. Sudbø, D. J. Krajnovich, H. S. Kwok, Y. R. Shen, and Y. T. Lee, *Ann. Rev. Phys. Chem.*, **30**, 379 (1979), and reference therein.

2) R. D. McAlpine and D. K. Evans, *Adv. Chem. Phys.*, **60**, 31 (1985).

3) A. Yokoyama, K. Yokoyama, and G. Fujisawa, *J. Chem. Phys.*, **100**, 6487 (1994).

4) S. Kato, Y. Makide, T. Tomonaga, and K. Takeuchi, *Laser Chem.*, **8**, 211 (1988).

5) K. Yokoyama, G. Fujisawa, and A. Yokoyama, *J. Chem. Phys.*, **102**, 7902 (1995).

6) D. Krajnovich, F. Huisken, Z. Zhang, Y. R. Shen, and Y. T. Lee, *J. Chem. Phys.*, **77**, 5977 (1982).

7) Y. Ishikawa and S. Arai, *Chem. Phys. Lett.*, **103**, 68 (1983).

8) Y. Ishikawa and S. Arai, *Bull. Chem. Soc. Jpn.*, **57**, 681 (1984).

9) D. W. Setser, T. S. Lee, and W. C. Danen, *J. Phys. Chem.*, **89**, 5799 (1985).

10) Aa. S. Sudbø, P. A. Schulz, E. R. Grant, Y. R. Shen, and Y. T. Lee, *J. Chem. Phys.*, **70**, 912 (1979).

11) Aa. S. Sudbø, P. A. Schulz, Y. R. Shen, and Y. T. Lee, *J. Chem. Phys.*, **69**, 2312 (1978).

12) A. Yokoyama, K. Yokoyama, and G. Fujisawa, *J. Chem. Phys.*, **101**, 10602 (1994).

13) A. Yokoyama, K. Yokoyama, and G. Fujisawa, *Chem. Phys. Lett.*, **237**, 106 (1995).

14) D. W. Lupo, M. Quack, and B. Vogelsanger, *Helv. Chim. Acta*, **70**, 129 (1987).

15) W. R. Wadt and P. J. Hay, *J. Chem. Phys.*, **82**, 284 (1985).

16) M. J. Frisch, M. Head-Gordon, G. W. Trucks, J. B. Foresman, H. B. Schlegel, K. Raghavachari, M. A. Robb, J. S. Binkley, C. Gonzalez, D. J. Defrees, D. J. Fox, R. A. Whiteside, R. Seeger, C. F. Melius, J. Baker, R. L. Martin, L. R. Kahn, J. J. P. Stewart, S. Topiol, and J. A. Pople, "Gaussian 90," Gaussian Inc., Pittsburgh (1990).

17) X. Zhao, Ph.D. Thesis, University of California, Berkeley.

18) J. C. Stephenson, S. E. Bialkowski, and D. S. King, *J. Chem. Phys.*, **72**, 1161 (1980).

19) B. E. Holmes and D. J. Rakestraw, *J. Phys. Chem.*, **96**, 2210 (1992).

20) R. N. Haszeldine, C. R. Pool, A. E. Tipping, and R. O'B. Watts, *J. Chem. Soc., Perkin Trans. 1*, **1976**, 513.

21) K. Sato, S. Tsunashima, T. Takayanagi, G. Fujisawa, and A. Yokoyama, *Chem. Phys. Lett.*, **242**, 401 (1995).

22) "Atlas of Mass Spectral Data," ed by E. Stenhagen, S. Abrahamsson, and F. W. McLafferty, Wiley, New York (1969).

23) R. E. Center and A. Mandl, *J. Chem. Phys.*, **57**, 4104 (1972).

24) D. Rapp and P. Englander-Golden, *J. Chem. Phys.*, **43**, 1464 (1965).

25) T. M. Miller and B. Bederson, *Adv. At. Mol. Phys.*,

13, 1 (1977).
26) "Kagakubinran," ed by the Chemical Society of Japan, Maruzen, Tokyo (1984).
27) T. Iwaoka, C. Kaneko, A. Shigihara, and H. Ichikawa, *J. Phys. Org. Chem.*, **6**, 195 (1993).
28) H. B. Schlegel and C. Sosa, *J. Phys. Chem.*, **88**, 1141 (1984).
29) L. Zhu, W. Chen, W. L. Hase, and E. W. Kaiser, *J. Phys. Chem.*, **9**, 311 (1993).
30) "Ab Initio Molecular Orbital Theory," ed by W. J. Hehre, L. Radom, P. v.R. Schleyer, and J. A. Pople, Wiley, New York (1986).